# Analytical Model for the Strain Analysis of Continuous Buried Pipelines in Geohazard Areas

# Analytical Model for the Strain Analysis of Continuous Buried Pipelines in Geohazard Areas

**Gregory C. Sarvanis[1] and Spyros A. Karamanos[1,2,*]**

Department of Mechanical Engineering, University of Thessaly, Volos, Greece

School of Engineering, The University of Edinburgh, Edinburgh, UK

## ABSTRACT

In geohazard areas, buried pipelines are subjected to permanent ground-induced deformations, which constitute major threats for their structural safety. Geohazards include seismic fault movement, liquefaction-induced lateral spreading, slope instability or soil subsidence, and are associated with the development of severe strains in the pipeline. Calculation of these strains is necessary for assessing pipeline integrity. In the present paper, an analytical methodology is presented that allows for simple and efficient pipeline strain analysis in geohazard areas. The methodology is compared with existing more elaborate analytical methodologies and finite element predictions. The analytical formulation results in closed form expressions and the model contributes to better understanding of buried pipeline behavior subjected to permanent ground-induced deformations. The proposed methodology is directly applicable to fault actions, but it can be also applicable to a wide range of geohazards. Furthermore, using this methodology, one may predict the strains developed in the pipeline wall due to ground-induced actions in a simple and efficiently manner and is suitable for the preliminary design of pipelines.

## KEYWORDS

Buried Pipeline, Pipeline Analysis, Geohazards, Pipeline Design, Local Buckling, Soil-Pipe Interaction.

## INTRODUCTION

Buried pipelines are often constructed in geohazard areas, crossing active seismic faults, liquefaction areas or slope instability regions, associated with the possible development of significant ground deformations. Avoiding these geohazard areas would be the safest option for pipeline alignment, but this option may not always be possible. In particular, in high-seismicity areas a large number of seismic faults often exist, which means that any pipeline alignment in this area will certainly cross a number of faults. Furthermore, the pipeline may cross areas prone to liquefaction or

* Corresponding author; email: spyros.karamanos@ed.ac.uk

mountainous areas with slope instabilities. In all those cases, the pipeline must be designed taking into account the additional stresses and deformations induced by the above ground movements.

The paper of Newmark and Hall [1] has been a pioneering publication in the area of pipeline stress analysis subjected to ground-induced actions, introducing an analytical model for calculating strains within a buried pipeline crossing a tectonic fault. Continuing the work in [1], Kennedy *et al*. [2] developed an analytical model, ignoring pipeline bending stiffness, while Wang and Yeh [3] improved this methodology accounting for pipeline bending stiffness. In subsequent publications, Takada *et al*. [4], Karamitros *et al*. [5] and Trifonov *et al*. [6] [7] presented analytical and semi-analytical methodologies for analyzing buried pipelines crossing seismic faults. More recently, together with the development of rigorous finite element models a simplified analytical formulation has been proposed in a series of publications by Vazouras *et al*. [8] [9] [10] and Zhang *et al*. [11] for describing pipeline deformation under strike-slip fault action. In addition to the above research publications, analytical expressions for the response of buried pipelines under permanent ground-induced deformations have been gradually introduced in design provisions of several standards and design recommendations [12], [13] and [14]. For an overview of seismic design of buried pipelines, with emphasis on steel water pipelines, the reader is referred to the recent paper by Karamanos *et al*. [15].

Permanent ground actions are characterized generally by the differential motion of two adjacent soil blocks crossed by the pipeline, and they can be categorized in two major groups. The first group includes the cases with the same soil resistance at the two moving parts of the soil, herein referred to as “symmetric” cases. The second group refers to cases with different soil properties and resistance at the two soil parts, referred to as “non-symmetric” cases. Strike-slip faults are examples of symmetric cases because the transverse (horizontal) soil resistance at both sides of the fault is practically the same. On the other hand, normal and oblique fault crossings are “non-symmetric” cases because vertical soil resistance is quite different in the upward and downward direction. One may also consider lateral spreading as a non-symmetric case, because of the different resistance against pipeline motion offered by the liquefied and the non-liquefied soil.

In the present paper, a novel analytical methodology is proposed for the calculation of strains induced in the pipeline due to permanent ground deformation. The methodology follows a simple and efficient formulation, which leads to closed-form expressions for the maximum strain induced into the pipeline. The model offers an efficient tool for understanding their mechanical behavior and can be employed for preliminary design of buried pipelines subjected to ground-induced actions. The work has been part of European research project GIPIPE, sponsored by the European Commission, aimed at examining the effects of permanent ground deformations on buried steel pipelines [16]. The model is based on an assumed-shape function for pipeline deformation suitable for symmetric and no symmetric soil resistance which leads to closed-form expressions for the bending and membrane strain in the pipeline wall. A key step towards developing the model is the calculation of the length of deformed pipeline shape, using an equivalent static model. The proposed analytical methodology is compared with simplified and rigorous finite element models, as well as with more elaborate analytical methodologies. The proposed methodology is directly applicable to fault crossing areas, but it can be readily adjusted for the case of landslide or liquefaction-induced action.

## PROPOSED METHODOLOGY

The problem under consideration can be stated schematically in Fig. 1a. The buried pipeline crosses a discontinuity plane in the ground at angle $\beta$. The discontinuity plane can be a tectonic fault, the edge of a landslide or the interface between liquefied and non-liquefied soil. For the sake of simplicity, in the following this "discontinuity plane" will be referred to as "fault plane" or "fault". The main requirement for applying this methodology is that the permanent ground deformation induces tensile (stretching) deformation of the pipe (crossing angle $\beta > 0$), together with bending. Furthermore, the proposed methodology may not describe accurately post-buckling pipeline configurations.

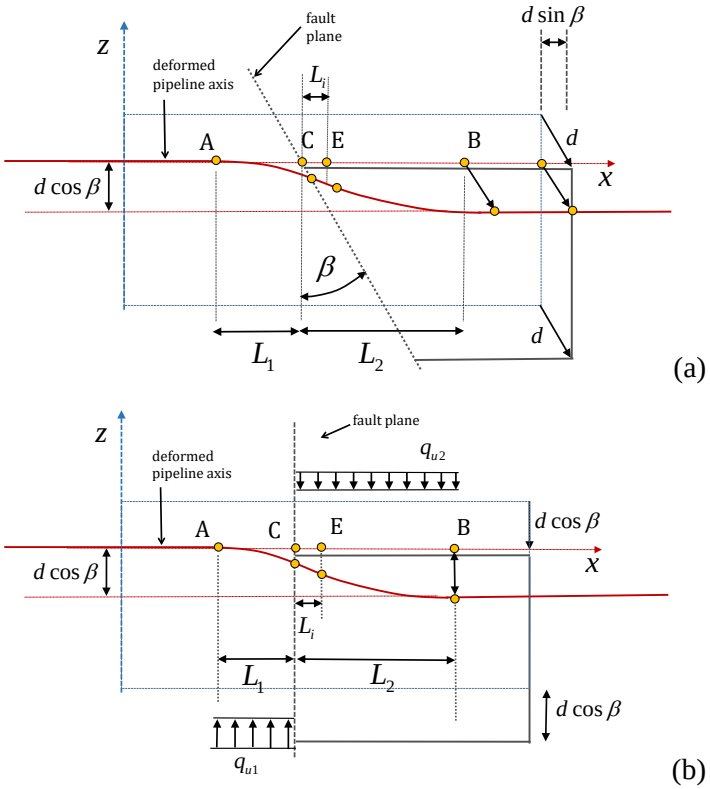


Fig. 1: (a) Schematic representation of ground-induced deformation of pipeline. (b) Deformation of pipeline considering only the transverse component of ground-induced deformation.

The ground on the right side of the fault moves parallel to the fault direction, by an amount $d$ with respect to the ground on the left side. Due to this differential ground motion, the pipeline is subjected to both bending and stretching, obtaining an S-shape configuration shown in Fig. 1a. The lengths $L_1$ and $L_2$ in Fig. 1 correspond to the lengths of the deformed S-shape of the pipeline in each side of the fault, while $L_i$ is the distance of the inflection point (point where the curvature changes sign) from the fault plane. The development of the present analytical model is based on the adoption of an assumed-shape function for the deformed pipeline shape, enhancing the concept of a simple analytical model presented

recently by Vazouras *et al*. [10]. It is noted that the model presented in [10], is applicable to the case of symmetric soil resistance only. In addition, the assumed-shape function in [10] did not satisfy the zero curvature condition at the two ends of the deformed pipeline segment and, furthermore, a systematic way to calculate the length of the deformed pipeline has not been provided. The present methodology, described in detail below, enhances the model proposed in [10] to account for the above deficiencies.

### Strain and curvature at the deformed pipeline

The first step in the development of the analytical methodology is the decomposition of ground motion in a transverse and a longitudinal (axial) component. Fig. 1b refers to the transverse deformation of the pipeline, due to the lateral component of ground displacement equal to $d\cos\beta$, and stems from Fig. 1a excluding the longitudinal component. The longitudinal component will be examined at a later part of this paragraph. The proposed assumed shape function for the transverse displacement $u(x)$ is expressed as follows:

$$u(x)=\begin{cases}\hat{d}(L_1+L_i)\cos\beta\left[1+\left[\frac{1}{4}\sin\left(\frac{\pi x}{L_1+L_i}\right)\right]-\left(\frac{x}{L_1+L_i}\right)\right] & 0\le x\le L_1+L_i \\ \hat{d}(L_2-L_i)\cos\beta\left[1+\left[\frac{1}{4}\sin\left(\frac{\pi(-x+L_1+L_i)}{L_2-L_i}\right)\right]-\left(\frac{x+L_2-L_1-2L_i}{L_2-L_i}\right)\right] & L_1+L_i\le x\le L\end{cases} \tag{1}$$

where $\hat{d}$ is the normalized ground displacement $\hat{d}=d/(L_1+L_2)$. The two ends of the S-shape pipe segment are located at $x=0$ and $x=L_1+L_2$. Eq. (1) can be written in a dimensionless form replacing the variable $x$ with the dimensionless coordinate $\xi$, where $\xi=x/(L_1+L_2)$, and the definition of ratios $\alpha$ and $\alpha_i$, ($\alpha=L_1/L_2$, $\alpha_i=L_i/L_2$). In this case the two ends of the S-shape pipe segment are located at $\xi=0,\ (x=0)$ and $\xi=1,\ (x=L_1+L_2)$. The choice of Eq. (1) is based on the requirement that the second derivative of the deformed shape (curvature) should attenuate towards the two ends, and reach a zero value at $x=0$ and $x=L$ . Eq. (1) can be written in dimensionless form as follows:

$$u(\xi)=\begin{cases}\frac{\alpha+\alpha_i}{\alpha+1}\left[1+\left[\frac{1}{4}\sin\left(\pi\frac{\alpha+1}{\alpha+\alpha_i}\xi\right)\right]-\left(\frac{\alpha+1}{\alpha+\alpha_i}\xi\right)\right] & 0\le\xi\le\xi_i \\ \frac{1-\alpha_i}{\alpha+1}\left[1+\left[\frac{1}{4}\sin\left(\pi\frac{(\alpha+\alpha_i)-(\alpha+1)\xi}{1-\alpha_i}\right)\right]-\left(\frac{(\alpha+1)\xi+1-(\alpha+2\alpha_i)}{1-\alpha_i}\right)\right] & \xi_i\le\xi\le 1\end{cases} \tag{2}$$

where $u(\xi)=u(x)/d\cos\beta$ and $\xi_i=(L_1+L_i)/(L_1+L_2)$

This assumed-shape function $u(x)$ is applicable to both symmetric and non-symmetric conditions with respect to the fault plane, and satisfies the continuity conditions (displacement and curvature) at the inflection point and is capable of describing deformation of pipe material in both the elastic and the plastic region. In addition, it satisfies the following boundary conditions at the two ends of the S-shaped segment under consideration.

$$\left|u(0)-u(L_1+L_2)\right| = d\cos\beta \tag{3}$$

$$u''(0) = u''(L_1+L_2) = 0 \tag{4}$$

where $(\bullet)''$ denotes double differentiation in terms of $x$.

The bending curvature $k$, due to the imposed lateral soil displacement $d\cos\beta$, can be readily computed by double differentiation of Eq. (1) as follows:

$$k(x) = -\frac{d^2u(x)}{dx^2} = \begin{cases} \dfrac{\pi^2\hat{d}\cos\beta}{4(L_1+L_i)}\sin\left(\dfrac{\pi x}{(L_1+L_i)}\right) & 0\le x\le L_1+L_i \\ \dfrac{\pi^2\hat{d}\cos\beta}{4(L_2-L_i)}\sin\left(\dfrac{\pi(L_1+L_i-x)}{(L_2-L_i)}\right) & L_1+L_i\le x\le L \end{cases} \tag{5}$$

Using the normalized coordinate $\xi$ along the pipeline axis, and the length ratios $\alpha$ and $\alpha_i$, the corresponding normalized curvature, $k(\xi)=k(x)/k_N$ is given by Eq. (6), where $k_N=\left(\hat{d}\cos\beta\right)/\left(L_1+L_2\right)$.

$$k(\xi) = \begin{cases} \dfrac{\pi^2(\alpha+1)}{4(\alpha+\alpha_i)}\sin\left(\pi\dfrac{\alpha+1}{\alpha+\alpha_i}\xi\right) & 0\le\xi\le\xi_i \\ \dfrac{\pi^2(\alpha+1)}{4(1-\alpha_i)}\sin\left(\pi\dfrac{\alpha+\alpha_i-(\alpha+1)\xi}{1-\alpha_i}\right) & \xi_i\le\xi\le 1 \end{cases} \tag{6}$$

In the case of symmetric soil resistance lengths $L_1$ and $L_2$ are equal, $L_1=L_2$, the inflection point is located at the fault plane, which is in the middle point of the pipe segment $\left(L_i=0\right)$, and the pipeline deformed shape is anti-symmetric. In Fig. 2, the proposed shape function $u(\xi)$, expressed by Eq. (2) and the corresponding curvature function $k(\xi)$, expressed by Eq. (6), are plotted for length ratio values $\alpha=0.166$ and $\alpha_i=0.111$. Furthermore, in Fig. 3, the proposed shape function $u(\xi)$ and the corresponding curvature function $k(\xi)$ are plotted for length ratio values $\alpha=1$ and $\alpha_i=0$.

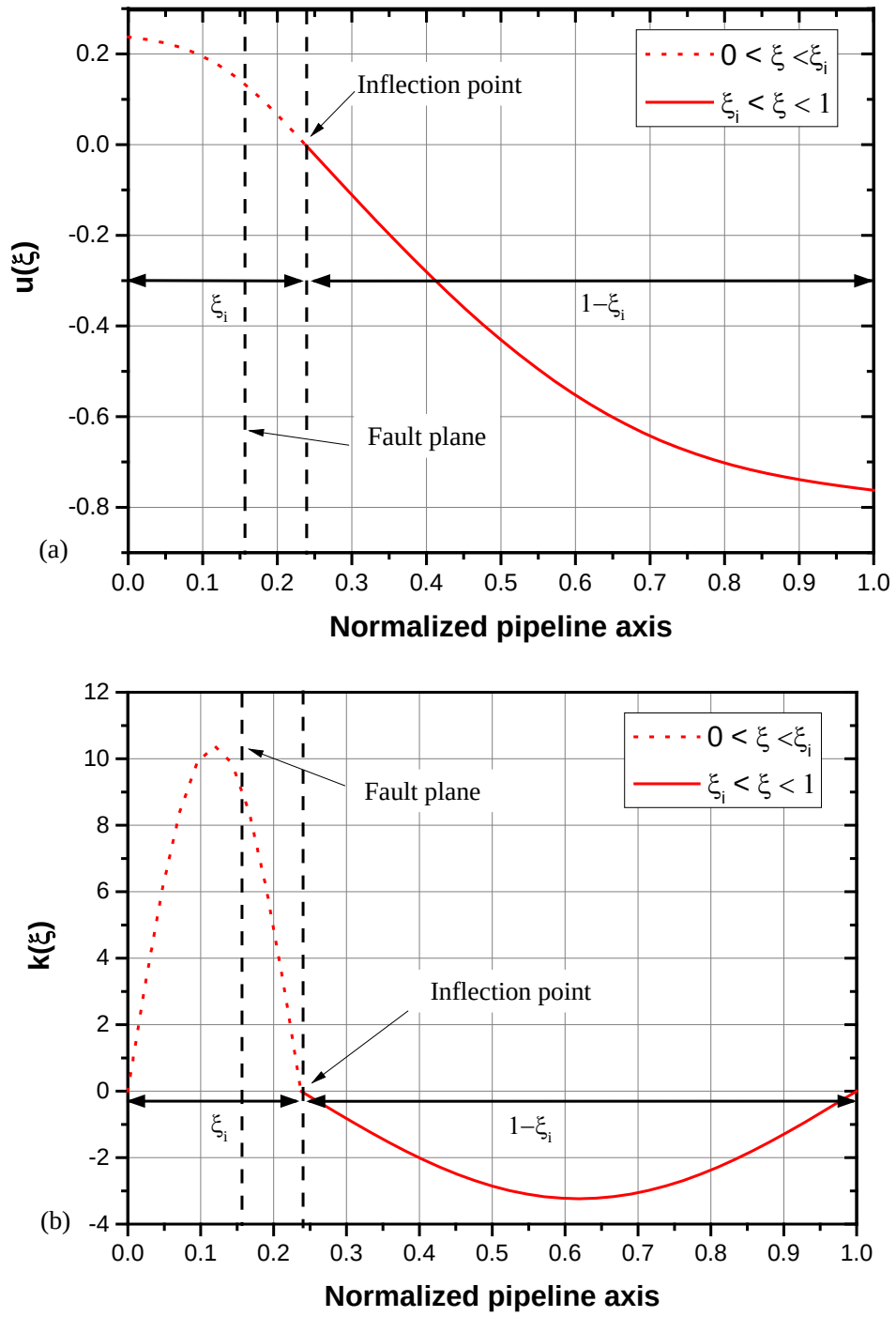


Fig. 2: Proposed shape function $u(\xi)$, as expressed by Eq. (2) and the corresponding curvature $k(\xi)$, as expressed by Eq. (6), are plotted for length ratio values $\alpha = 0.166$ and $\alpha_i = 0.111$ (non-symmetric case).

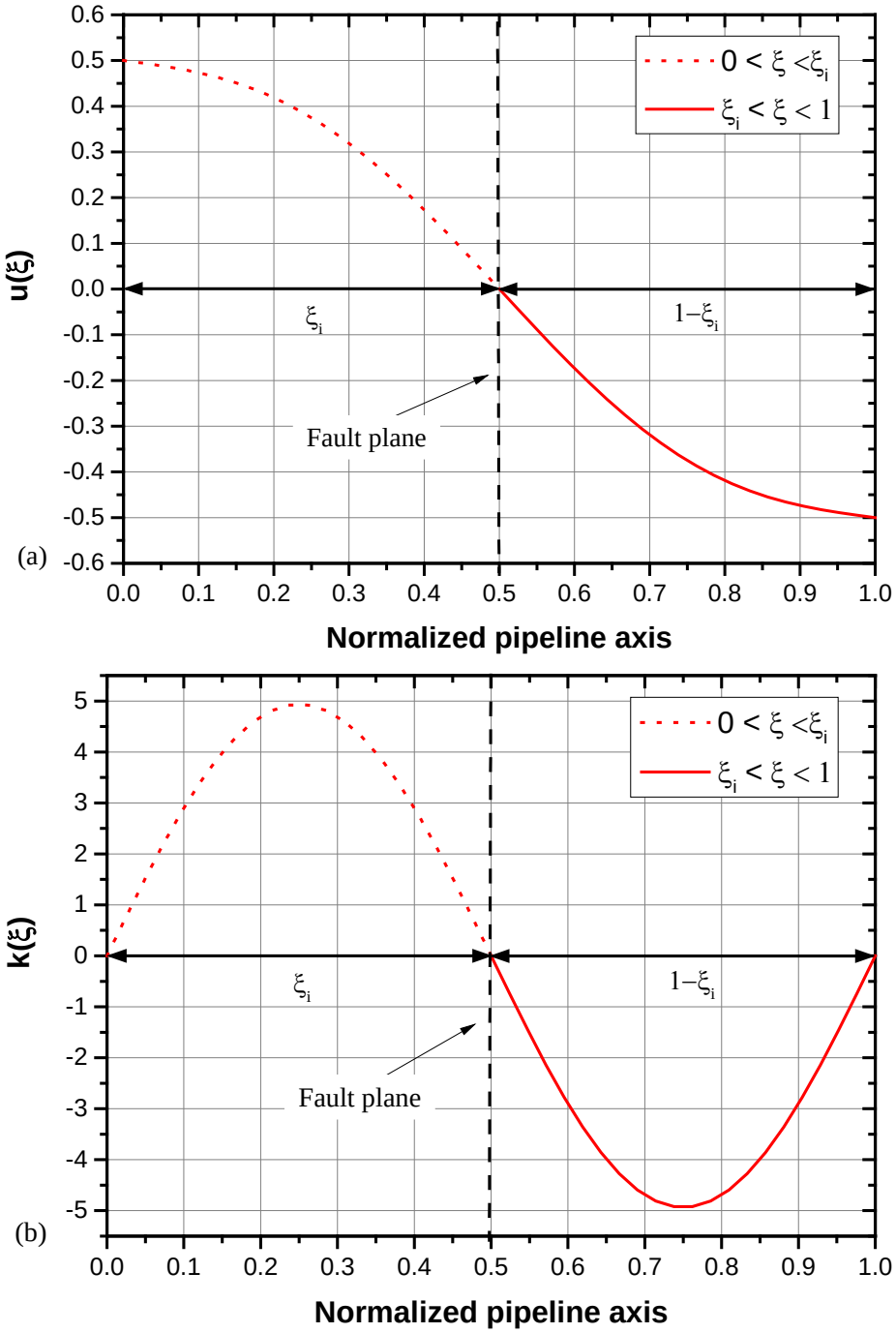


Fig. 3: Proposed shape function $u(\xi)$ expressed by Eq. (2) and the corresponding curvature $k(\xi)$, expressed by Eq. (6), are plotted for length ratio values $\alpha = 1$ and $\alpha_i = 0$ (symmetric case).

Neglecting cross-sectional distortion or ovalization, the bending strain $\varepsilon_b(x)$ of the deformed pipe due to transverse imposed displacement $d\cos\beta$ can be obtained along the pipe from beam bending theory as follows:

$$\varepsilon_b(x) = -\frac{d^2u(x)}{dx^2}\frac{D}{2} = \begin{cases} \dfrac{\pi^2 D\hat{d}\cos\beta}{8(L_1+L_i)}\sin\left(\dfrac{\pi x}{(L_1+L_i)}\right) & 0 \le x \le L_1+L_i \\ \dfrac{\pi^2 D\hat{d}\cos\beta}{8(L_2-L_i)}\sin\left(\dfrac{\pi(L_1+L_i-\mathrm{x})}{(L_2-L_i)}\right) & L_1+L_i \le x \le L \end{cases} \tag{7}$$

The maximum bending strain $\varepsilon_b$ of the deformed pipe can be obtained in terms of maximum bending curvature $k_{\max}$ as follows:

$$\varepsilon_b = \frac{D}{2}k_{\max} = \frac{\pi^2 D}{8(L_1+L_i)}\hat{d}\cos\beta \tag{8}$$

In addition to bending, the pipeline is also subjected to significant axial stretching (membrane strain) due to the change of its length. The elongation $\Delta_1$ of the pipeline segment within the length $L$ under consideration, due to transverse displacement $u(x)$ can be expressed as follows:

$$\Delta_1 = \int_0^L \sqrt{1+u'^2}\,dx - L \tag{9}$$

Furthermore, the axial displacement of the pipeline $v(x)$ associated with the longitudinal component of ground motion, equal to $d\sin\beta$, induces further stretching within this pipe segment and should be added to total stretching deformation. It is assumed that this axial displacement is linearly distributed along the pipeline segment under consideration, described by the following equation:

$$v(x) = \frac{d\sin\beta}{L}x, \quad 0 \le x \le L \tag{10}$$

and the corresponding total elongation of the pipe segment is equal to

$$\Delta_2 = d\sin\beta \tag{11}$$

Combining the above and considering end effects of the pipeline segment, the total elongation of the pipeline segment under consideration can be expressed as follows:

$$\Delta = \left(\int_0^L \sqrt{1+u'^2}\,dx - L\right) + d\sin\beta - \delta \tag{12}$$

In Eq. (12), the first term in the parenthesis refers to the elongation $\Delta_1$ (stretching) due to transverse displacement, the second term refers to the increase of the length $\Delta_2$ due to the oblique direction of soil movement, while the third term accounts for the axial flexibility of the adjacent parts of the pipeline outside the length $L$ under consideration, represented by an axial shortening displacement $\delta$.

Considering compatibility at the two pipe ends of the pipe segment, the following equation is obtained that relates the total elongation $\Delta$ with the end flexibility displacement $\delta$.

$$\frac{EA}{L}\Delta = \overline{K}_t \frac{\delta}{2} \tag{13}$$

or equivalently

$$\Delta = \omega\delta \tag{14}$$

where

$$\omega = \frac{\overline{K}_t L}{2EA} \tag{15}$$

In the above equations, $A$ is the cross sectional area of the pipe, $E$ is Young's modulus of the steel pipe material and $\overline{K}_t$ expresses the axial stiffness of the straight part of the pipeline outside the S-shaped length $L$. An expression for $\overline{K}_t$ has been developed in [10] using an analytical methodology, as follows:

$$\overline{K}_t = \sqrt{EAk_s} \tag{16}$$

where $k_s$ is the stiffness of soil resistance per pipe unit length in the pipe axial direction and can be obtained by relevant standards and design recommendations. More details on the development of Eq. (16) can be found in [10] [16].

The total axial membrane strain $\varepsilon_m$ is assumed uniform within the pipe segment under consideration, and can be readily calculated from Eq. (12) as follows:

$$\varepsilon_m = \frac{\Delta}{L} = \frac{1}{L}\int_0^L \sqrt{1+u'^2}\,dx - 1 + \frac{d\sin\beta}{L} - \frac{\delta}{L} \tag{17}$$

Using the following series expansion to linearize the integral term,

$$\sqrt{1+u'^2} = 1 + \frac{1}{2}u'^2 + \cdots \tag{18}$$

and using Eq. (9) and Eq. (13), the membrane strain in Eq. (17) becomes:

$$\varepsilon_m = \left(\frac{(32+\pi^2)}{64}\hat{d}^2\cos^2\beta + \hat{d}\sin\beta\right)\left(\frac{\omega}{\omega+1}\right) \tag{19}$$

There exist two extreme cases related to the axial stiffness $\overline{K}_t$ of the straight part of the pipeline outside the S-shaped length. The first case refers to very stiff end conditions, corresponding to large values of $\overline{K}_t$. Assuming $\overline{K}_t \to \infty$ in Eq. (13) the requirement of real-valued total elongation $\Delta$ leads to $\delta = 0$, so that $\Delta = \Delta_1 + \Delta_2$. The other extreme case

refers to very flexible end conditions, corresponding to zero values of $\overline{K}_t$; assuming $\overline{K}_t = 0$, Eq. (15) results in $\omega = 0$, and therefore on readily obtains $\Delta = 0$ and $\varepsilon_m = 0$.

The total strain in the pipeline is the sum of membrane strain $\varepsilon_m$ in Eq. (19) and the bending strain $\varepsilon_b$ in Eq. (8). For the crossing configuration under consideration (positive values of $\beta$), membrane strain $\varepsilon_m$ is always tensile, while the bending strain $\varepsilon_b$ can be either tensile or compressive, depending on the direction of bending. Therefore, the maximum tensile strain $\varepsilon_T$ is expressed as follows:

$$\varepsilon_T = \varepsilon_b + \varepsilon_m \tag{20}$$

and the maximum compressive strain $\varepsilon_c$ is

$$\varepsilon_c = \varepsilon_b - \varepsilon_m \tag{21}$$

Using Eq. (8) and Eq. (19) and setting the maximum compressive strain $\varepsilon_c$ equal to the critical compressive strain $\varepsilon_{Cu}$, Eq. (21) results in the following quadratic equation for the critical ground displacement $\hat{d}_{cr}$, which expresses the condition for the onset of local buckling:

$$\left[\left(\frac{(32+\pi^2)}{64}\right)\left(\frac{\omega}{\omega+1}\right)\cos^2\beta\right]\hat{d}_{cr}^2 - \left[\frac{\pi^2 D}{8(L_1+L_i)}\cos\beta - \left(\frac{\omega}{\omega+1}\right)\sin\beta\right]\hat{d}_{cr} + \left[\varepsilon_{Cu}\right] = 0 \tag{22}$$

It is interesting to notice that the solution of Eq. (22) provides the ground displacement at which the pipe cross section reaches the critical (ultimate) compressive strain $\varepsilon_{Cu}$ and that existence of real-valued solution in Eq. (22) depends on the sign of the discriminant of the quadratic polynomial on the left-hand side of Eq. (22). After some straightforward mathematical manipulations, this discriminant $\mathcal{D}$ can be written as a quadratic expression in terms of $\tan\beta$, as shown below:

$$\mathcal{D} = C_3\left(\tan\beta\right)^2 + 2C_2C_3\left(\tan\beta\right) - 4C_1\varepsilon_{Cu} + C_2{}^2 \tag{23}$$

where $C_1$, $C_2$ and $C_3$ are given by the following equations:

$$C_1 = \left(\frac{(32+\pi^2)}{64}\right)\left(\frac{\omega}{\omega+1}\right) \tag{24}$$

$$C_2 = \frac{\pi^2 D}{8(L_1+L_i)} \tag{25}$$

$$C_3 = -\left(\frac{\omega}{\omega+1}\right) \tag{26}$$

The critical compressive strain $\varepsilon_{Cu}$ can be reached only if $\mathcal{D} \geq 0$, so that Eq. (22) has real-valued solutions. Therefore, imposing the requirement of negative discriminant [see Eq. (27) below], one may specify in a fault-crossing situation the range of crossing angle $\beta$ values, for which the pipeline may not exhibit local buckling:

$$\mathcal{D} < 0 \tag{27}$$

## Length of deformed pipeline

In the analytical model described in the previous paragraph, the value of lengths $L_1$ and $L_2$ of the S-shape of the pipeline, as well as the value of length $L_i$ should be determined. It is recalled that $L_1$ and $L_2$ are the distances between the fault and the zero curvature (and zero bending moment) end points of the S-shape length, while length $L_i$ is the distance between the fault and the inflection point of the pipeline S-shape (Fig. 1).

To calculate these lengths in a systematic way, for the general case of non-symmetric soil resistance conditions, an equivalent static elastic model is developed, which is based primarily on a detailed description of pipeline transverse deflection, shown in Fig. 1b. The distributed loads $q_{u1}$ and $q_{u2}$ are the maximum soil resistances per unit length on the left part (length $L_1$) and on the right part (length $L_2$) on either side of the fault. These distributed transverse loads are assumed constant along the lengths $L_1$ and $L_2$, despite the fact that they depend on transverse displacements and are decreasing away from the fault.

In the present formulation, it is assumed that $L_2$ is larger than $L_1$ ($L_2 \geq L_1$), which means that the soil resistance $q_{u1}$ is larger than soil resistance $q_{u2}$. Assuming elastic response of the pipe, the transverse deformation in Fig. 1b can be decomposed in two bending deformation patterns, expressed through the bending moment diagrams (a) and (b) of Fig. 4. More specifically, the bending moment diagram (a) is the result of the differential movement of the supports in the transverse direction, which represents the permanent soil movement at the two sides of the fault, while the bending moment diagram (b) is the result of distributed loading, representing soil resistance.

The bending moments at the two ends of diagram (a), namely $M_A$ and $M_B$, can be computed in terms of ground displacement $d$ as follows, using standard beam analysis tools [17]:

$$M_A = -\frac{6EJd\cos\beta}{(L_1+L_2)^2} \tag{28}$$

$$M_B = \frac{6EJd\cos\beta}{(L_1+L_2)^2} \tag{29}$$

where $E$ is the Young's Modulus, $J$ is the moment of inertia of the pipe cross section ( $J = \pi D^3 t/8$ ) and $D$ is the mean pipe diameter.

Furthermore, the end bending moments $M'_A$ and $M'_B$ of diagram (b) in Fig. 4 can be computed from the following equations [17]:

$$M'_A = \frac{1}{3}[r_1 + l_2 - 2l_1 - 2r_2] \tag{30}$$

$$M'_B = \frac{1}{3}[r_2 + l_1 - 2l_2 - 2r_1] \tag{31}$$

where expressions for $r_1$, $r_2$, $l_1$ and $l_2$ are given in Eq. (32) to Eq. (36) below:

$$l_1 = \frac{1}{3}q_{u1}L_1^2\gamma_1(1-0.75\gamma_1) \tag{32}$$

$$l_2 = -\frac{1}{3} q_{u2} L_2^2 \gamma_2 (1 - 0.75\gamma_2) \tag{33}$$

$$r_1 = \frac{1}{3} q_{u1} L_1^2 (1.5 - 2\gamma_1 + 0.75\gamma_1^2) \tag{34}$$

$$r_2 = -\frac{1}{3} q_{u2} L_2^2 (1.5 - 2\gamma_2 + 0.75\gamma_2^2) \tag{35}$$

$$\gamma_1 = \frac{L_1}{L_1 + L_2} \quad \gamma_2 = \frac{L_2}{L_1 + L_2} \tag{36}$$

In the above expressions, the values of $q_{u1}$ and $q_{u2}$ can be obtained from relevant standards and design recommendations for pipeline design [12] [13] [14].

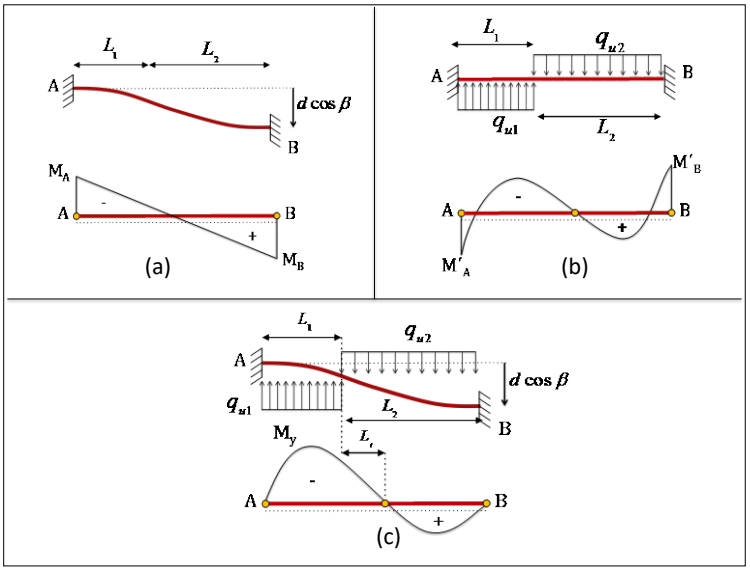


Fig. 4: Equivalent static model for the calculation of lengths $L_1$ and $L_2$ of the deformed pipeline shape.

Deformation patterns (a) and (b) are superimposed, resulting in pattern (c) of Fig. 4c. In the later configuration, the bending moments at the two ends A and B are enforced to be zero, so that

$$M_A + M'_A = 0 \tag{37}$$

$$M_B + M'_B = 0 \tag{38}$$

Using Eq. (28) to Eq. (36), and after some mathematical manipulations, Eq. (37) and Eq. (38) can be written in the following form:

$$27.8L_1^4 q_{u1} + 111L_1^3 L_2 q_{u1} - L_1^2 L_2^2 (-167q_{u2} - 333q_{u1}) - 111L_1 L_2^3 q_{u2} - 27.8L_2^4 q_{u2} = 6000EJd\cos\beta \tag{39}$$

$$27.8L_1^4 q_{u1} + 111L_1^3 L_2 q_{u1} - L_1^2 L_2^2 (167q_{u1} + 333q_{u2}) - 111L_1 L_2^3 q_{u2} - 27.8L_2^4 q_{u2} = -6000EJd\cos\beta \tag{40}$$

One may note that Eq. (39) and Eq. (40), allow for the computation of $L_1$ and $L_2$ for a given value of ground displacement $d$.

Combining Eq. (39) and Eq. (40) one can readily obtain the following equation that relates the length ratio $\alpha = L_1/L_2$, with the soil resistance ratio $b = q_{u1}/q_{u2}$:

$$b = \frac{1+3\alpha}{\alpha^2(3+\alpha)} \tag{41}$$

A graphically representation of Eq. (41) is shown in Fig. 5.

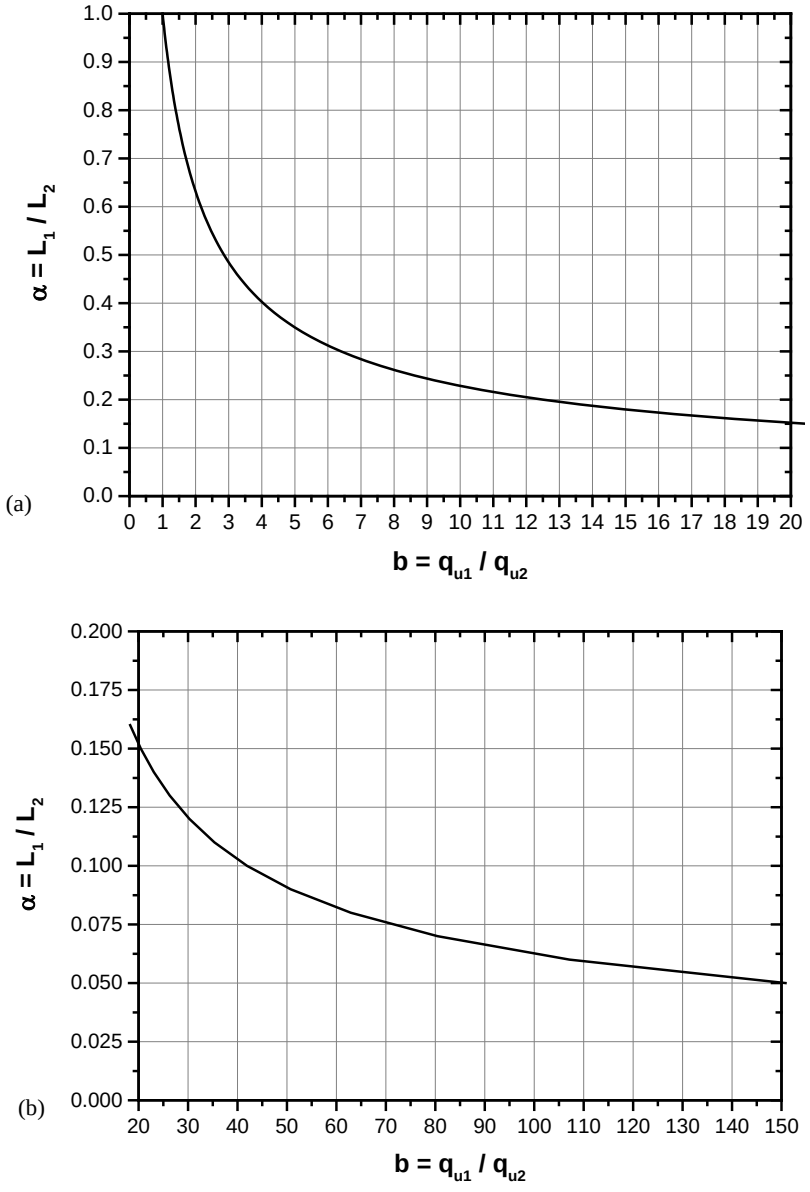


Fig. 5: Dependence of length ratio $(\alpha = L_1/L_2)$ on soil resistance ratio $b = q_{u1}/q_{u2}$; (a) diagram for *b* values between 0 and 20, (b) diagram for *b* values between 20 and 150.

A key assumption is made at this point: upon first yielding of pipeline material, the values of lengths $L_1$ and $L_2$ remain constant. The main argument in support of this assumption is that, upon yielding at a specific location, deformation will start localizing at this point, so that the general shape of the pipeline in terms of lengths $L_1$, $L_2$ and $L_i$ may not change significantly. The accuracy of this assumption is verified in a later section of the present paper.

To implement the above assumption in the present analytical formulation, the maximum bending moment in diagram (c) is calculated from the following expression:

$$M_{\max} = \left( V_{\mathrm{A}} - \frac{12EJd\cos\beta}{L^3} \right) x_{\max} - q_{u1} \frac{x_{\max}^2}{2} \tag{42}$$

where $V_A$ is the shear force at point (A) corresponding to the bending moment diagram (b) of Fig. 4b, given by Eq. (43), the second term in brackets of Eq. (42) is the shear force of Fig. 4a, while $x_{\max}$ is the position of the maximum bending moment with respect to point (A) of the Diagram (c) in Fig. 4c and is given by Eq. (44):

$$V_A = \frac{1}{L}\left( M'_B - M'_A + q_{u1} L_1 (L_2 + \frac{L_1}{2}) - q_{u2} \frac{{L_2}^2}{2} \right) \tag{43}$$

$$x_{\max} = \frac{V_{\mathrm{A}} - \dfrac{12EJd\cos\beta}{L^3}}{q_{u1}} \tag{44}$$

Setting the value of $M_{max}$ equal to the yield moment $M_y$ of the pipe cross-section ($M_y = \sigma_y \frac{\pi}{4} D^2 t$), Eq. (42) leads to another equation that relates $L_1$ and $L_2$ with the ground displacement $d_y$ that correspond to pipeline first yielding. More specifically, using Eq. (41), and after some straight forward mathematical manipulations, Eq. (42) results in the following expression for $d_y$:

$$\frac{d_y}{D} = \left( \frac{\sigma_y}{E} \right) \left( \frac{t}{D} \right) \left( \frac{D\sigma_y}{q_{u2}} \right) F(a) \tag{45}$$

where function $F(a)$ can be written as follows:

$$F(\alpha) = \frac{2.3562(3+a)\left(\frac{1}{3}+a\right)^2 (1+a)^{15}}{\left\{1+a\left[6+a(4+a)\right]\right\}^4} \tag{46}$$

and is plotted in Fig. 6.

Finally, combining Eq. (39) and Eq. (40) and setting the ground displacement $d\cos\beta$ equal to $d_y$, the value of length $L_1$ can be computed by the following equation:

$$L_1 = \sqrt{\alpha}\left(\frac{24 d_y EJ}{q_{u2} + q_{u1}}\right)^{1/4} \tag{47}$$

Subsequently, length $L_2$ can be readily computed from the definition of length ratio $\alpha$.

$$L_2 = \frac{L_1}{\alpha} \tag{48}$$

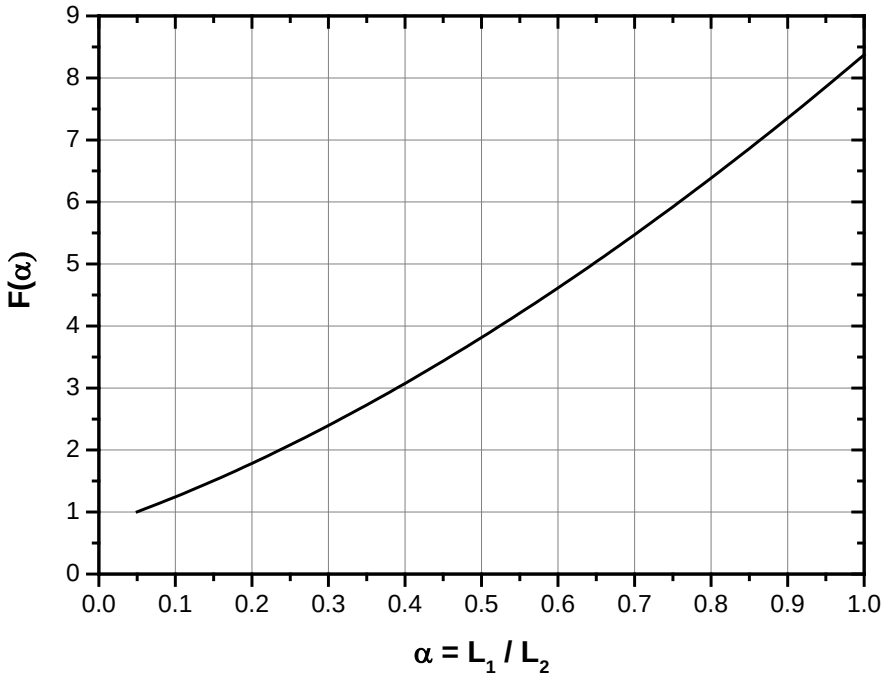


Fig. 6: Graphical representation of function $F(\alpha)$, with respect to length ratio $\alpha$.

The distance $L_i$ between the fault and the inflection point can be simply calculated by applying static equilibrium in the moment diagram (c) of Fig. 4c. This results in the following quadratic equation with respect to $L_i$:

$$\left[\frac{q_{u2}}{2}\right]L_i^2 + \left[V_A - \frac{12EJd}{L^3} - (\alpha+1)\,q_{u2}\,L_1\right]L_i + \left[\frac{L_1^2}{2}q_{u2}(1+\alpha)\right] = 0 \tag{49}$$

In the case of symmetric soil resistance, $L_1 = L_2 = L/2$, $L_i = 0$ and $q_{u1} = q_{u2} = p_u$. Therefore, Eq.(39) and Eq.(40) obtain the following simple form:

$$L^4 p_u = 192 EJd\cos\beta \tag{50}$$

Eq. (50) can be solved in terms of the total length value $L = 2\ L_1$. Therefore, the length $L$ is given by the following equation:

$$L = 2\left(\frac{12 d_y EJ}{p_u}\right)^{1/4} \tag{51}$$

Inserting Eq. (51) into Eq. (42), which expresses the maximum value of bending moment diagram (c) in Fig. 4c, a simpler form for the maximum bending moment can be obtained:

$$M_{\max} = 0.433\sqrt{EJ p_u d \cos\beta} \tag{52}$$

Setting the value of $M_{\max}$ equal to the yield moment $M_y$ of the pipe cross-section ( $M_y = \sigma_y \frac{\pi}{4} D^2 t$ ), Eq. (52) leads to an equation that relates $L_1$ and $L_2$ with the ground displacement $d_y$ that corresponds to pipeline first yielding. Finally, in the case of symmetric soil resistance, the value of $F(\alpha)$ is equal to 42/5, so that Eq. (45), which expresses the yield displacement becomes:

$$\frac{d_y}{D} = \frac{42}{5}\left(\frac{\sigma_y}{E}\right)\left(\frac{t}{D}\right)\left(\frac{D\sigma_y}{p_u}\right) \tag{53}$$

## Summary of the proposed methodology

The above methodology is summarized in Table 1. Using this methodology, one may predict in simple manner and with good accuracy the deformed shape of the pipeline subjected to permanent soil deformations and the corresponding strains at the pipe wall.

Table 1: Summary of the proposed strain analysis methodology

Given the geometric and material properties of the pipe $(D,\ t, E, \sigma_y)$, the maximum soil resistances of the surrounding soil $(q_{u1},\ q_{u2},\ t_u)$, the imposed ground displacement *d*, and the angle $\beta$ at which the pipeline crosses the discontinuity plane:

(1) Calculate the soil resistance ratio $b = q_{u1}/q_{u2}$ .

(2) Calculate the length ratio $\alpha = L_1/L_2$ from Fig. 5 using the soil resistance ratio $b = q_{u1}/q_{u2}$ .

(3) Find parameter $F(a)$ from Fig. 6 using the length ratio $\alpha = L_1/L_2$ .

(4) Calculate the ground displacement $d_y$ corresponding to first yielding of the pipe cross section.

$$\frac{d_y}{D} = \left(\frac{\sigma_y}{E}\right)\left(\frac{t}{D}\right)\left(\frac{D\sigma_y}{q_{u2}}\right)F(a)$$

(5) Compute the characteristic lengths of the deformed S-shape of the pipeline $L_1$, $L_2$ and $L_i$:

$$L_1 = \sqrt{\alpha}\left(\frac{24 d_y EJ}{q_{u2}+q_{u1}}\right)^{1/4}$$

$$L_2 = \frac{L_1}{\alpha}$$

and $L_i$ from the solution of quadratic equation (49).

(6) Calculate the maximum bending strain $\varepsilon_b$ and the membrane strain $\varepsilon_m$:

$$\varepsilon_b = \frac{\pi^2 D}{8(L_1+L_i)}\hat{d}\cos\beta$$

$$\varepsilon_m = \left(\frac{(32+\pi^2)}{64}\hat{d}^2\cos^2\beta + \hat{d}\sin\beta\right)\left(\frac{\omega}{\omega+1}\right)$$

where $\hat{d} = d/(L_1+L_2)$ and $\omega$ is calculated from Eq. (15).

(7) Calculate the maximum tensile strain $\varepsilon_T$ and the maximum compressive strain $\varepsilon_C$; compare with the corresponding strain limits:

$$\varepsilon_T = \varepsilon_b + \varepsilon_m \le \varepsilon_{Tu}$$

$$\varepsilon_C = \varepsilon_b - \varepsilon_m \le \varepsilon_{Cu}$$

## BRIEF PRESENTATION OF FINITE ELEMENTS MODELS USED FOR PIPELINE ANALYSIS

In previous works, several finite element methodologies have been developed to model the effects of ground-induced actions on buried pipelines, and a relevant overview can be found in [15]. There exist two levels of finite element modeling of pipeline analysis under ground-induced actions. The first level (Level 1) is widely used in pipeline design practice against geohazards, whereas the second level (Level 2), employs a three-dimensional continuum approach for the surrounding soil and a shell-type description for the pipe and is used only in special cases, where increased computational accuracy is necessary. In the following, a short description of these numerical approaches is offered.

### Level 1 Modeling

In this level of analysis, the pipe is modeled with special-purpose beam-type finite elements, often referred to as “pipe elements” or “elbow elements”. Those special-purpose “pipe elements” account for the presence of hoop stress and strain due to pressure, and have the capability of describing cross-sectional ovalization, which is necessary for the accuracy of the finite element solution, especially at pipeline bends. This methodology is employed for simulating permanent ground-induced actions on pipelines, such as faults, landslides and lateral spreading at several design projects. The finite element mesh near discontinuities (e.g. fault plane) should be fine enough, so that gradients of stress and strains are accurately simulated.

The pipe material is elastic-plastic, considering strain hardening effects. Furthermore, the ground surrounding the pipeline is modeled with appropriate springs, attached on the pipe nodes and directed in the axial and the two transverse directions as shown in Fig. 7. The springs follow a nonlinear “law” representing the load-deformation behavior of the soil, including possible slip of the pipe through the soil, resulting in nonlinear load-deflection curves. Expressions for axial and transverse springs are offered in the ALA Guidelines [12] or NEN 3650 [13], according to the soil type.

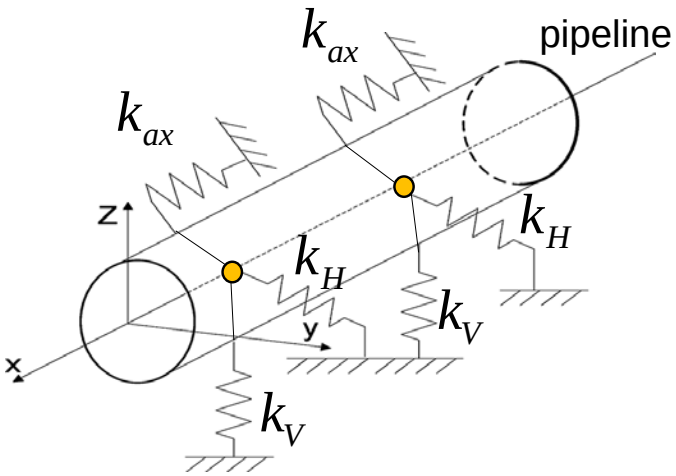


Fig. 7: Level 1 of pipeline modelling; pipe (beam-type) finite elements and soil springs attached to pipeline nodes in the three principal directions.

In the present paper, the "elbow elements" from program Abaqus [18] have been used for pipeline modelling at this level. These are special-purpose three-node non-linear elements with the capability of describing cross-sectional ovalization and pressure effects. The models have a length of about 1000 m so that the end conditions of the deformed segment of pipeline may not affect the state of deformation at the critical region. Furthermore, the pipe material has been modeled as elastic-plastic using appropriate material data.

### Level 2 Modeling

This second level of analysis offers the capability of rigorous calculations using three-dimensional continuous models that employ shell elements for simulating the pipe and three-dimensional solid elements for describing the surrounding soil. The basic idea behind this model is the consideration of an elongated prismatic model where the steel pipeline is embedded in two adjacent soil blocks, separated by the discontinuity plane (e.g. fault plane, edge of landslide or lateral spreading). Ground-induced movement is imposed keeping one soil block fixed, while imposing a displacement pattern at the external nodes of the second block. A fine mesh is employed for both the pipeline and the soil at the vicinity of the discontinuity plane, where maximum stresses and strains are expected. The relative movement of the two blocks is considered to occur gradually within a narrow zone of width, equal to about one pipe diameter, to avoid numerical problems. The mechanical behavior of soil material is described through a Mohr-Coulomb model, available in almost all finite element programs.

Fig. 8 shows the finite element model used in the present study for a 36-in-diameter pipeline crossing a strike-slip fault at angle $\beta = 20^o$. Four-node reduced integration shell elements are employed for modelling the pipeline and eight-node reduced-integration "brick" elements are employed to simulate the soil. The total length of the model is equal to 65 pipe diameters and special-purpose springs are used at the two ends of the model for simulating pipeline continuity [10]. More details on this approach are offered in [8] [9] [10][19].

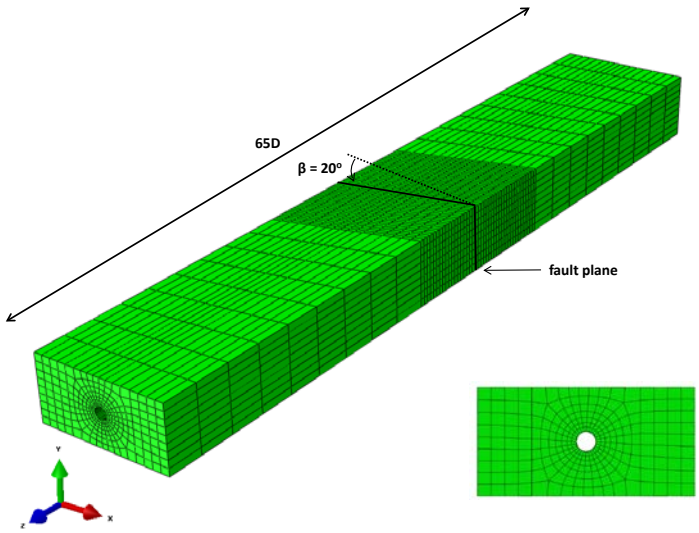


Fig. 8: Finite element model in Abaqus for level 2 simulation of soil-pipe interaction.

## VALIDATION OF THE PROPOSED ANALYTICAL METHODOLOGY AGAINST EXISTING ANALYTICAL AND NUMERICAL RESULTS

Four cases are analyzed with the proposed analytical methodology and compared with available analytical methodologies and finite element results. Three cases with symmetric soil resistance (strike-slip faults) are examined first for different pipes and soil conditions, and compared with numerical results from level 1 and level 2 models, as well as with the predictions of an elaborate semi-analytical methodology proposed in [5], that requires an iterative solution scheme. Moreover, a case with non-symmetric soil resistance is analyzed and compared with numerical results from level 1 models. Furthermore, the validity of the assumption that length $L$ remains unchanged upon first yielding of the pipeline is examined. Prior to yielding the position of maximum strain is not fixed, which means that length $L$ is not constant. Beyond pipe yielding, the position of maximum strain remains does not change significantly for increasing ground-induced displacement, which means that length $L$ can be considered constant. The deformed pipeline shape and the distribution of axial strains along the pipe axis are plotted for different fault displacement values *d* before and after yielding of pipe cross section.

### Case 1

The first case concerns a 1066-mm-diameter (42 in.) X60 steel pipeline $\left(\sigma_y = 415\ MPa\right)$, with thickness equal to 14.27 mm (0.562 in.), crossing a strike-slip fault, with cohesionless soil conditions. A comparison between the proposed methodology and finite element results from level 1 modelling is conducted. Properties of the cohesionless soil (sand) and geometric parameters of the pipe are summarized in Table 2. The strike-slip fault is considered to be crossed at two different fault angles $\beta$, namely 0° and 10° degrees. The analysis is performed for fault displacement equal to 1 and 2 meters for each angle $\beta$.

This is a symmetric case, where the total length $L$ of the curved pipe segment is computed from Eq. (47) equal to 27.6 m, lengths $L_1$ and $L_2$ are equal to the half of the total length $L$, $L_1 = L_2 = 13.8\ m$ and length $L_i$ is zero. The strain results from the finite element analysis and the proposed analytical expressions Eq. (20) and Eq. (21) are presented in Table 3 and Table 4for the two values of angle $\beta$. The comparison between Eq. (1) and the deformed shape of the pipe from finite element analysis is depicted in Fig. 9 and Fig. 11 for crossing angles $\beta = 0^o$ and $\beta = 10^o$, respectively, while the distribution of axial strains along the pipe axis is shown in Fig. 10 and Fig. 12 for the two angles $\beta$. The comparison of maximum axial strains and length $L$ between finite element analysis and the present analytical methodology indicates good agreement.

According to the finite element analysis for crossing angle $\beta = 0^o$ the pipe cross section reaches first yielding at fault displacement equal to 0.54 m, while the corresponding fault displacement value predicted by Eq. (53) is 0.46 m. In Fig. 13 the distribution of axial strains along the pipe, obtained from numerical analysis, is shown for different fault displacements $d$ before and after yielding of the pipe. The numerical results indicate that the position of maximum strain does not change significantly after first yield of the pipe, and the length $L$ of the deformed pipeline segment remains practically constant.

Table 2: Soil parameters and geometric properties (Cases 1, 2, 3).

| | Case 1 | Case 2 | Case 3 |
|---|---|---|---|
| φ | $34^O$ | $36^O$ | $32^O$ |
| $K_O$ | 0.5 | 0.5 | 0.5 |
| γ (kg/m$^3$) | 1760 | 1800 | 1830 |
| $H_c$ (m) | 0.9 | 1.3 | 2.5 |
| D (mm) | 1066 | 914.4 | 914.4 |
| t (mm) | 14.27 | 11.91 | 11.91 |
| $p_u$ (kN/m) | 220 | 318.6 | - |
| $t_u$ (kN/m) | 22.7 | 40.5 | - |
| $y_u$ (m) | 0.005 | 0.003 | - |

Table 3: Comparison between proposed methodology and FEM results for angle $\beta$ equal to 0º (Case 1).

| | max tensile strain % | | max compressive strain % | |
|---|---|---|---|---|
| *d* (m) | present methodology | FEM | present methodology | FEM |
| 1 | 0.36 | 0.34 | 0.32 | 0.28 |
| 2 | 0.76 | 0.87 | 0.61 | 0.75 |

Table 4: Comparison between proposed methodology and FEM results for angle $\beta$ equal to 10º (Case 1).

| | max tensile strain % | | max compressive strain % | |
|---|---|---|---|---|
| *d* (m) | present methodology | FEM | present methodology | FEM |
| 1 | 0.50 | 0.47 | 0.18 | 0.18 |
| 2 | 1.03 | 0.94 | 0.32 | 0.29 |

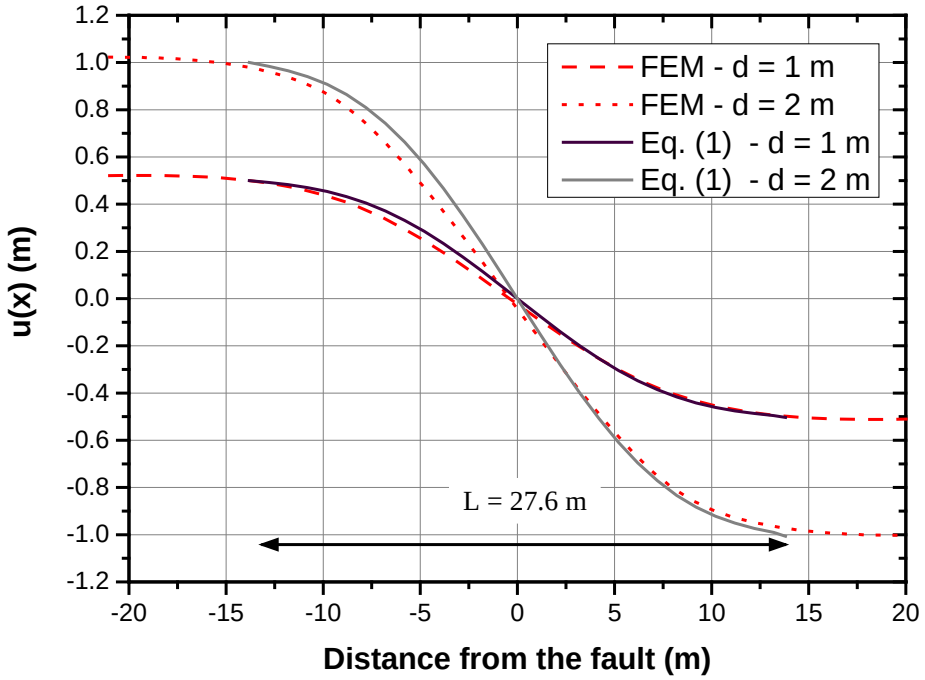


Fig. 9: Deformed pipeline shape; comparison between predictions of the present methodology and those from finite element model (level 1) for two values of fault displacement $d$ (Case 1, $\beta = 0^o$).

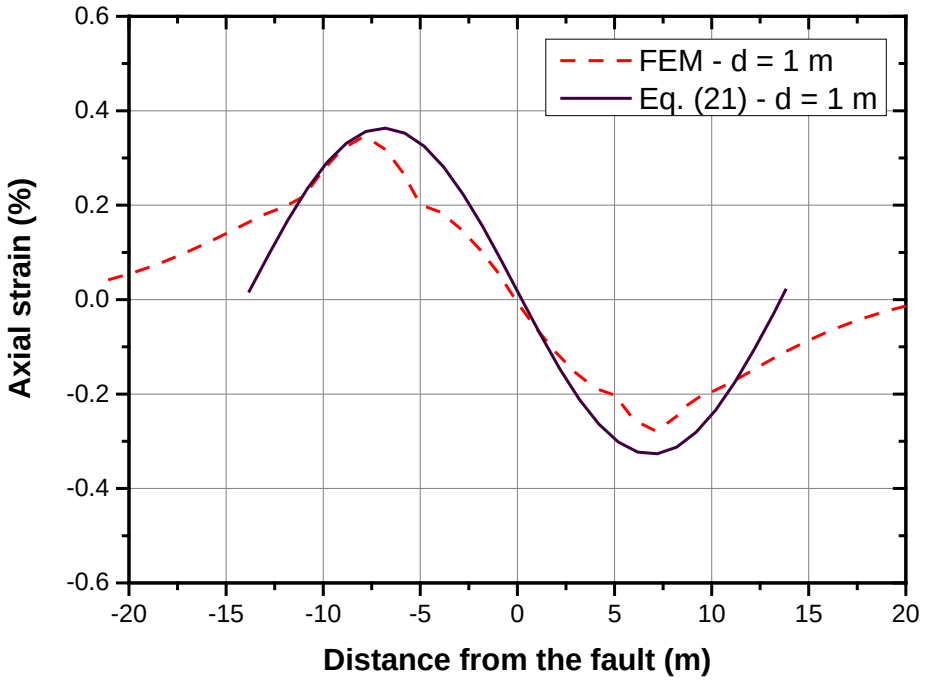


Fig. 10: Distribution of axial strains along the pipe; comparison between predictions of the present methodology and those from finite element models (level 1) for fault displacement $d = 1\,m$; (Case 1, $\beta = 0^o$).

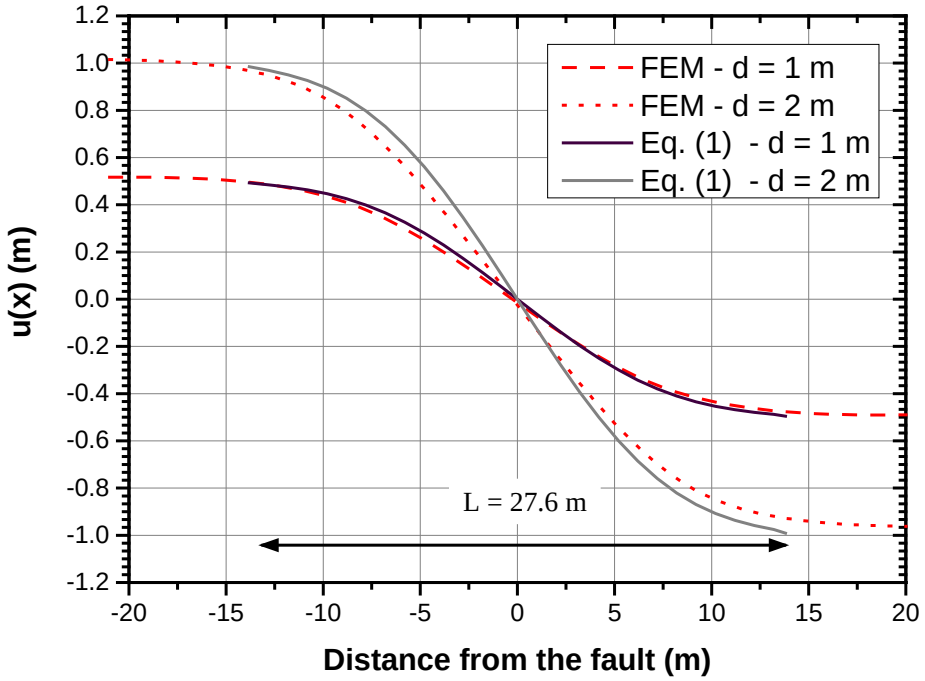


Fig. 11: Deformed pipeline shape; comparison between predictions of the present methodology and those from finite element models (level 1) for two values of fault displacement $d$ (Case 1, $\beta = 10^o$).

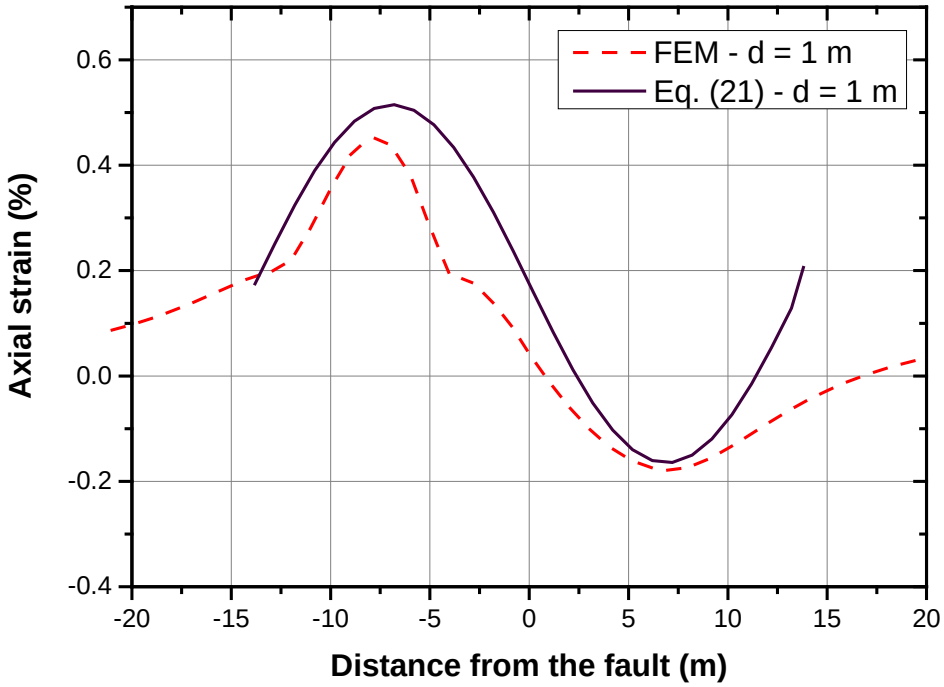


Fig. 12: Distribution of axial strains along the pipe axis, comparison between predictions of the present methodology and those from finite element models (level 1) for fault displacement $d = 1\,m$;(Case 1, $\beta = 10^o$).

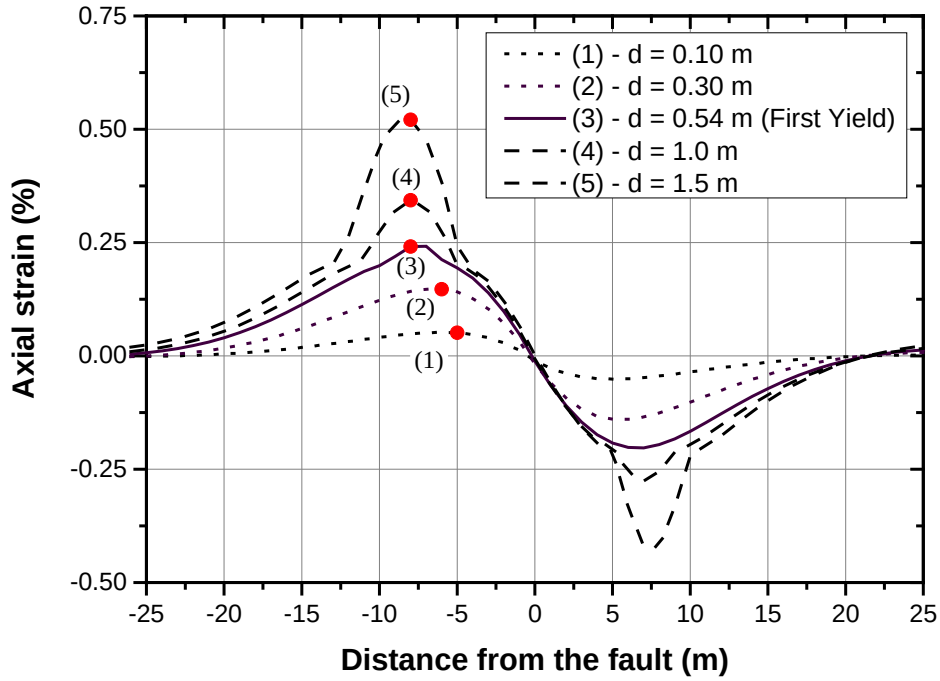


Fig. 13: Distribution of axial strains along the pipe for different values of displacement *d*; numerical finite element results (Case 1, $\beta = 0^o$).

A parametric analysis with respect to angle $\beta$ is conducted for this case to examine the vadility of Eq. (27). It is reminded that the solution of Eq. (22) provides the ground displacement at which the pipe compressive strain reaches the critical value $\varepsilon_{Cu}$. Furthermore existence of solution in Eq. (22) depends on the sign its discriminant and, therefore, on angle $\beta$. If the discriminant of Eq. (22) is negative, Eq. (22) has not real-valued solution and, hence, the pipe will not reach the critical compressive strain $\varepsilon_{Cu}$ for any value of imposed displacement $d$.

In the present case according to Eq. (27), angle $\beta$ must be larger than 5.4° $\left(\beta \geq 5.4^o\right)$ in order for the pipe not to reach the critical compressive strain $\varepsilon_{Cu}$, which in this case was taken equal to 0.5% according to EN 1998-4 standard [20]. Fig. 14 plots the maximum compressive strain in the pipe, in terms of the applied ground displacement for different values of angle $\beta$. The numerical results indicate that if the angle $\beta$ is larger than approximately 5°, the pipe will not reach the critical compressive strain $\varepsilon_{Cu}$ and will not exhibit local buckling, an observation consistent with the aforementioned analytical prediction.

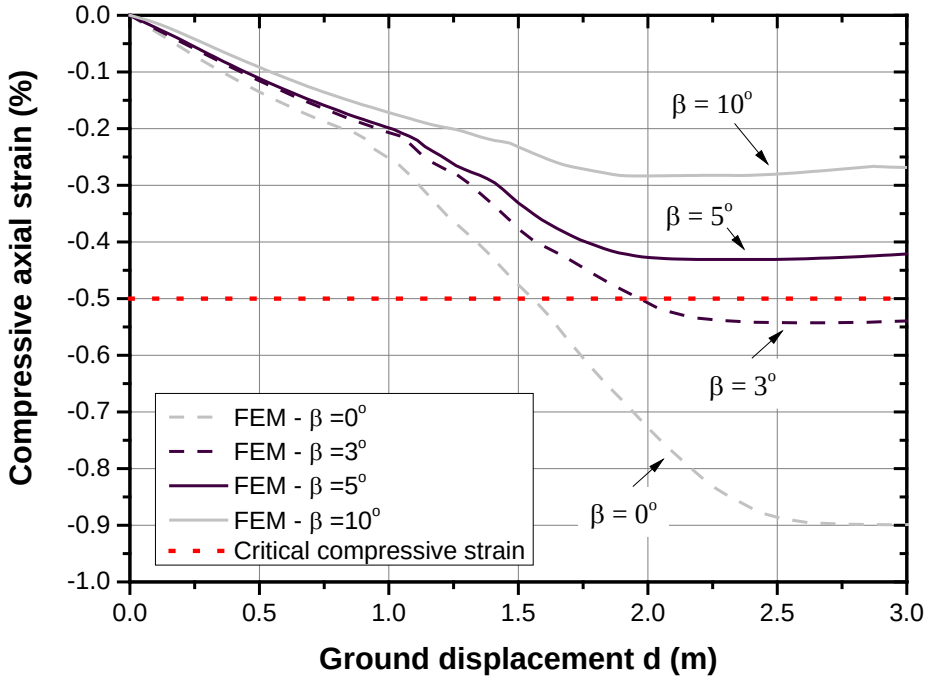


Fig. 14: Maximum compressive strain in terms of imposed ground displacement for different values of angle $\beta$ (Case 1).

### Case 2

The second case refers to a high-pressure gas pipeline, with diameter equal to 914.4-mm (36 in.), thickness equal to 11.91 mm (0.469 in.), made of X65 steel $\left(\sigma_y = 490\ MPa\right)$. The pipeline crosses a strike-slip fault with cohesionless soil conditions. The soil properties, the geometric and the material parameters of the pipe are tabulated in Table 2. The predictions of the proposed methodology, are compared with the predictions of finite element analysis (level 1) and the semi-analytical results reported in [5] for two different angles $\beta$ , namely 30º and 60º, as shown in Table 5 and in Table 6 for two values of crossing angle $\beta$. The length $L$ of the curved pipe segment is computed from Eq. (47) equal to 18.95 m, the length $L_1$ and $L_2$ are equal to the half of the total length $L$, $L_1 = L_2 = 9.80\ m$ and the length $L_i$ is equal to zero. The comparison between Eq. (1) and deformed shape obtained from FE analysis is depicted to Fig. 15 for crossing angle $\beta$ equal to 30º. According to the finite element results, the pipe cross section enters the plastic zone at fault displacement equal to 0.47 m, while the corresponding prediction of Eq. (53) is 0.33 m. In Fig. 16 the distribution of axial strains along the pipe is shown for different fault displacement value *d* before and after yielding of pipe cross section. The finite elements results also indicate that the configuration deformed pipeline segment in terms of length $L$ does not change significantly after the first yield of pipe cross section.

Table 5: Comparison between proposed methodology, finite element models and analytical results from ref. [5] for angle $\beta$ equal to 30º (Case 2).

| | max tensile strain % | | |
|---|---|---|---|
| *d* (m) | present methodology | Karamitros *et al*. [5] | FEM |
| 0.914 (1D) | 1.19 | 1.25 | 1.46 |
| 1.371 (1.5D) | 1.81 | 1.70 | 1.85 |

Table 6: Comparison between proposed methodology, finite element modelling and analytical results from ref.[5] for angle $\beta$ equal to 60º (Case 2).

| | max tensile strain % | | |
|---|---|---|---|
| *d* (m) | present methodology | Karamitros *et al*. [5] | FEM |
| 0.914 (1D) | 1.48 | 1.52 | 1.57 |
| 1.371 (1.5D) | 2.23 | 2.50 | 2.25 |

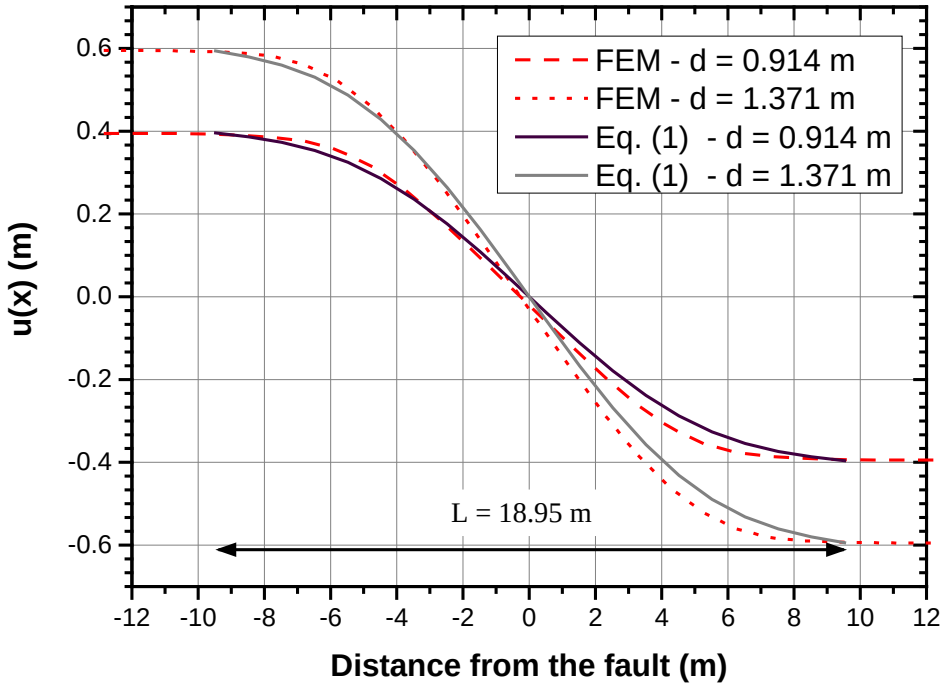


Fig. 15: Deformed pipeline shape, comparison between the predictions of the present methodology and those from finite element models (level 1) for two values of fault displacement $d$ (Case 2, $\beta = 30^o$).

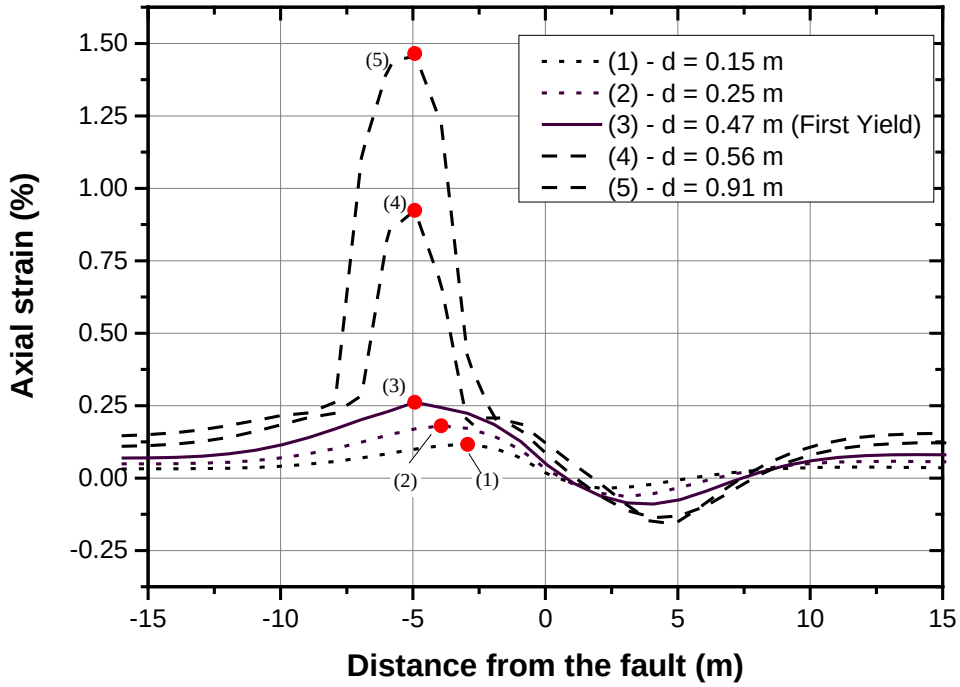


Fig. 16: Distribution of axial strains along the pipe for different values of displacement *d*; numerical finite element results (Case 2, $\beta = 30^o$ ).

### Case 3

The third case with symmetric soil resistance refers to a 914.4 mm-diameter (36 in.), X65 steel pressurized pipeline $\left(\sigma_y = 485\ MPa\right)$. Pipe thickness is 11.91 mm (0.469 in.) and internal pressure is 50 bar, while the soil properties and the geometric parameters of the pipe are presented in Table 2. Moreover a dilation angle equal to zero is assumed in this case. The pipeline crosses a strike-slip fault at angle $\beta = 20^o$ and a comparison between the proposed methodology and rigorous finite element analysis (level 2) is conducted. The length $L$ of the curved pipe segment is computed from Eq. (47) equal to 18.5 m, the length $L_1$ and $L_2$ are equal to the half of the total length $L$, $L_1 = L_2 = 9.25\ m$ and the length $L_i$ is equal to zero. The results from the rigorous finite element analysis and the proposed analytical methodology are presented and compared in Table 7. The comparison indicates also a very good agreement between analytical and numerical results in terms of tensile axial strains, while in the case of compressive strains the comparison indicates a diversion between analytical and numerical results. This diversion is attributed to the assumption of uniform distribution of axial stretching and was observed only in this case. In Fig. 17, the deformed shape from the rigorous finite element model is presented for fault displacement equal to 2.0 m.

Table 7: Comparison between proposed methodology and level 2 finite element modelling (Case 3, $\beta = 20^o$).

| | max tensile strain % | | max compressive strain % | |
|---|---|---|---|---|
| d (m) | present methodology | FEM | present methodology | FEM |
| 1 | 0.96 | 0.82 | 0.30 | 0.17 |
| 2 | 1.99 | 2.09 | 0.57 | 0.08 |

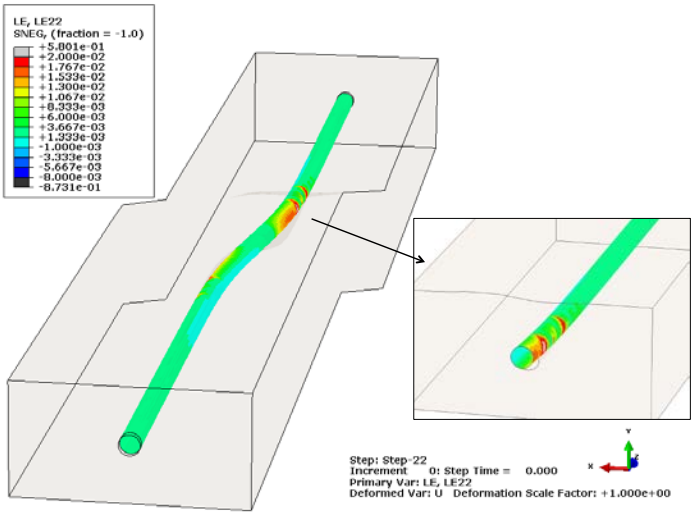


Fig. 17: Deformed shape of pipeline, for fault displacement equal to 2.0 m (Case 3, $\beta = 20^o$).

### Case 4

The fourth case, which is a real case of a buried gas pipeline crossing a seismic fault, refers to non-symmetric soil resistance, where a 1219-mm-diameter (48 in.), X65 steel pipeline $\left(\sigma_y = 485\ MPa\right)$ with 17.1 mm (0.673 in.) thickness, with embedment depth equal to 1.6 meters, crosses a normal fault with dip-angle equal to 70º, which implies a value equal to 20º for the angle $\beta$. The soil properties in terms of the corresponding soil resistances according to ALA Guidelines [12] are presented in Table 8 . The characteristic lengths $L_1$, $L_2$ and $L_i$ of the deformed shape of the pipeline according to Eq. (47), Eq. (48) and Eq. (49) are computed equal to $L_1 = 5.08\,\text{m}$ and $L_2 = 37.50\,\text{m}$ and $L_i = 15.42\,\text{m}$, respectively. The results from the finite element analysis (level 1) and the proposed analytical methodology are presented and compared in Table 9. The comparison indicates a very good agreement between analytical predictions and numerical results.

Table 8: Soil parameters (Case 4).

| | |
|---|---|
| $q_u$ upwards | 45 kN/m |
| $q_u$ downwards | 1100 kN/m |
| $t_u$ axial | 35 kN/m |
| $y_u$ upwards | 0.162 |
| $y_u$ downwards | 0.183 |
| $y_u$ axial | 0.005 |

Table 9: Comparison between proposed methodology and Level 1 finite element model (Case 4).

| | max tensile strain % | | max compressive strain % | |
|---|---|---|---|---|
| d (m) | present methodology | FEM | present methodology | FEM |
| 2 | 0.88 | 0.93 | 0.00 | 0.10 |
| 2.5 | 1.11 | 1.27 | 0.00 | 0.01 |

## Case 5

The fifth case also refers to a non-symmetric soil resistance, where a 914.4-mm-diameter (36 in.), X65 steel pipeline $\left(\sigma_y = 490\ MPa\right)$ with 11.9 mm (0.469 in.) thickness, crosses a normal fault with dip-angle equal to 70°, which implies a value equal to 20° for the angle $\beta$. The soil properties in terms of the corresponding soil resistances according to ALA Guidelines [12] are presented in Table 10. The characteristic lengths $L_1$, $L_2$ and $L_i$ of the deformed shape of the pipeline according to Eq. (47), Eq. (48) and Eq. (49) are computed equal to $L_1 = 2.91\,\text{m}$ and $L_2 = 22.4\,\text{m}$ and $L_i = 6.22\,\text{m}$, respectively. The results from the finite element analysis (level 1) and the proposed analytical methodology are presented and compared in Table 11. The comparison indicates a very good agreement between analytical predictions and numerical results.

Table 10: Soil parameters (Case 5).

| | |
|---|---|
| $q_u$ upwards | 52 kN/m |
| $q_u$ downwards | 1360 kN/m |
| $t_u$ axial | 40.5 kN/m |
| $y_u$ upwards | 0.0022 |
| $y_u$ downwards | 0.100 |
| $y_u$ axial | 0.003 |

Table 11: Comparison between proposed methodology Karamitros *et al.* [5] methodology and Level 1 finite element model (Case 5).

| | max tensile strain % | | |
|---|---|---|---|
| d (m) | present methodology | Karamitros *et al*. [5] | FEM |
| 0.731 (0.8D) | 0.70 | 0.65 | 0.60 |
| 0.823 (0.9D) | 0.79 | 0.82 | 0.86 |

## CONCLUSIONS

A novel analytical methodology has been proposed for pipeline strain analysis subjected to permanent ground-induced actions in geohazard areas which results in closed-form expressions for pipeline deflection and strains. The predictions from this methodology have been found to compare very well with the results from other available numerical simuilations and analytical methodologies, for cases where the pipe is subjected to bending and tension (i.e. for crossing angle $\beta > 0$). The comparison has demonstrated that the proposed methodology can predict quite satisfactorily: (a) the length of the transversely deformed shape of the pipeline under symmetric and non-symmetric soil resistance, and (b) the maximum strains induced in the pipeline wall due to permanent ground deformation. The closed-form expressions of the proposed methodology introduce a novel, simple and efficient tool for strain analysis, for the preliminary design of buried steel pipelines against geohazard permanent actions.

## NOTATION

$A$ Cross sectional area of the pipe

$D$ Outer diameter of the pipe

$E$ Young's Modulus

$H_c$ Burial depth of the pipe

$J$ Inertia moment of the pipe cross section

$M_A$ Bending moment at location (A)

$M_B$ Bending moment at location (B)

$M_y$ Yield moment of the pipe cross section

$K_o$ Lateral earth pressure coefficient

$L$ Total length of the deformed shape of the pipeline

$L_i$ Distance between the fault and the inflection point

$L_1$ Distance of the fault and the end point with bending moment equal to zero

$L_2$ Distance of the fault and the end point with bending moment equal to zero

$V_A$ Shear force

$d$ Value of ground-induced displacement

$d_y$ Value of ground-induced displacement corresponding to pipeline first yielding

$k$ Pipeline bending curvature

$k_s$ Stiffness of soil resistance per pipe unit length in the pipe axial direction

$p_u$ Soil resistance per unit length in horizondal direction

$q_{u1}$ Soil resistance per unit length in vertical direction corresponding to length $L_1$

$q_{u2}$ Soil resistances per unit length in vertical direction corresponding to length $L_2$

$t$ Pipe thickness

$t_u$ Soil resistance per unit length in axial direction

$y_u$ Soil displacement corresponding to maximum soil resistance

$\Delta$ Total elongation (stretching) of pipe segment

$\beta$ Fault crossing angle

$\delta$ Flexibility displacement at pipe ends

$\varepsilon_b$ Maximum bending strain

$\varepsilon_m$ Axial membrane strain

$\varphi$ Internal angle of soil friction

## ACKNOWLEGMENT

The present research work has been partially supported by a financial grant of the European Commission through the Research Fund for Coal and Steel (RFCS), Contract No. RFSR-CT-20011-00027, “Safety of Buried Steel Pipelines Under Ground-Induced Deformations”, project acronym GIPIPE.

## REFERENCES

[1] Newmark N. M. and Hall W. J. (1975), “Pipeline design to resist large fault displacement”. *Proceedings of U.S. National Conference on Earthquake Engineering*, pp. 416–425.

[2] Kennedy, R. P., Chow, A. W. and Williamson, R. A. (1977), “Fault movement effects on buried oil pipeline”, *ASCE Journal of Transportation Engineering*, Vol. 103, pp. 617-633.

[3] Wang, L. R. L. and Yeh, Y. A. (1985), “A refined seismic analysis and design of buried pipeline for fault movement”, *Earthquake Engineering & Structural Dynamics*, Vol. 13, pp. 75-96.

[4] Takada, S., Hassani, N. and Fukuda, K. (2001), “A new proposal for simplified design of buried steel pipes crossing active faults”, *Earthquake Engineering and Structural Dynamics*, Vol. 30, pp.1243–1257.

[5] Karamitros, D. K., Bouckovalas, G. D., and Kouretzis, G. P. (2007), “Stress Analysis of Buried Steel Pipelines at

Strike-Slip Fault Crossings.", *Soil Dynamics & Earthquake Engineering*, Vol. 27, pp. 200-211.

[6] Trifonov, O. V. and Cherniy, V. P. (2010), "A semi-analytical approach to a nonlinear stress–strain analysis of buried steel pipelines crossing active faults.", *Soil Dynamics & Earthquake Engineering*, Vol. 30, pp. 1298-1308.

[7] Trifonov, O. V. and Cherniy, V. P. (2012), "Elastoplastic stress-strain analysis of buried steel pipelines subjected to fault displacements with account for service loads.", *Soil Dynamics & Earthquake Engineering*, Vol. 33, No. 1, pp. 54-62.

[8] Vazouras, P., Karamanos, S. A., and Dakoulas, P. (2010), "Finite Element Analysis of Buried Steel Pipelines Under Strike-Slip Fault Displacements", *Soil Dynamics and Earthquake Engineering*, Vol. 30, No. 11, pp. 1361–1376.

[9] Vazouras, P., Karamanos, S. A., and Dakoulas, P. (2012), "Mechanical behavior of buried steel pipes crossing active strike-slip faults", *Soil Dynamics and Earthquake Engineering*, Vol. 41, pp. 164–180.

[10] Vazouras, P., Dakoulas, P., and Karamanos, S. A. (2015), "Pipe-Soil Interaction and Pipeline Performance Under Strike-Slip Fault Movements", *Soil Dynamics and Earthquake Engineering*, Vol. 72, pp. 48-65.

[11] Zhang, L., Zhao, X., Yan, X., and Yang, X., (2016) "A new finite element model of buried steel pipelines crossing strike-slip faults considering equivalent boundary springs", *Engineering Structures*, Vol. 123 pp. 30-44.

[12] American Lifelines Alliance (2001), *Guidelines for the Design of Buried Steel Pipe*, Reston, VA.

[13] Nederlands Normalisatie-Instituut (2006), *Requirements for Pipeline Systems*, NEN 3650, Part-1: General, and Part-2: Steel Pipelines.

[14] American Society of Civil Engineers (1984), *Guidelines for seismic design of oil and gas pipeline systems.* Committee on Gas and Liquid Fuel Lifelines, Technical Council on Lifeline Earthquake Engineering, Reston, VA.

[15] Karamanos, S. A., Keil, B. and Card, R. J. (2014), "Seismic design of buried steel water pipelines.", *ASCE Pipelines Conference*, Portland, Oregon.

[16] Vazouras, P. *et al*. (2015)," *Safety of buried steel pipelines under ground-induced deformations"*, Final Report, GIPIPE project, Research Fund for Coal & Steel, European Commission, Brussels, Belgium.

[17] BETON KALENDER (1983), Verlag von Wilhelm Ernst and Sohn, Berlin.

[18] ABAQUS Users' Manual, Simulia, Pawtucket, Rhode Island, 2013.

[19] Sarvanis, G. C, Ferino, J., Karamanos, S. A., Vazouras, P., Dakoulas, P., Mecozzi, E. (2016), "Numerical Investigation and Experimental Verification of Pipe-Soil Interaction for Buried Pipelines Crossing Geohazard Areas", *26th International Ocean and Polar Engineering Conference*, ISOPE 2016, Rhodes, Greece.

[20] European Committee for Standardization (2006), *Eurocode 8: Design of structures for earthquake resistance –Part 4: Silos, tanks and pipelines*, EN 1998-4, Brussels, Belgium.